Hurricane and Severe Storm Sentinel

Scott Braun (Code 612) NASA/GSFC

Using the NASA Global Hawk and WB-57, the HS3 mission successfully overflew four Atlantic tropical cyclones in 2014, including two major hurricanes (4 Global Hawk flights over Edouard, 3 WB-57 flights over Gonzalo)

CPL & S-HIS look into the eye of Edouard during rapid intensification on Sept. 14-15

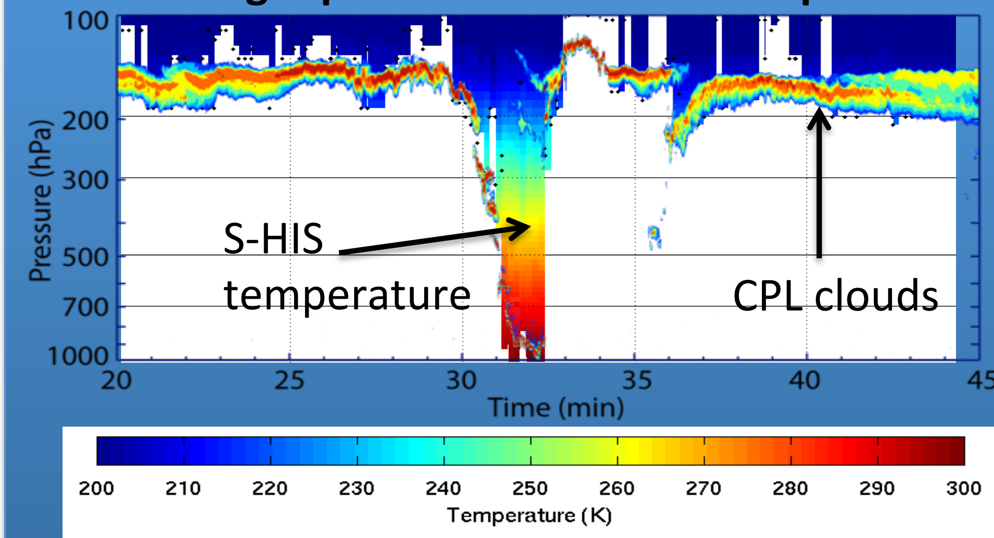

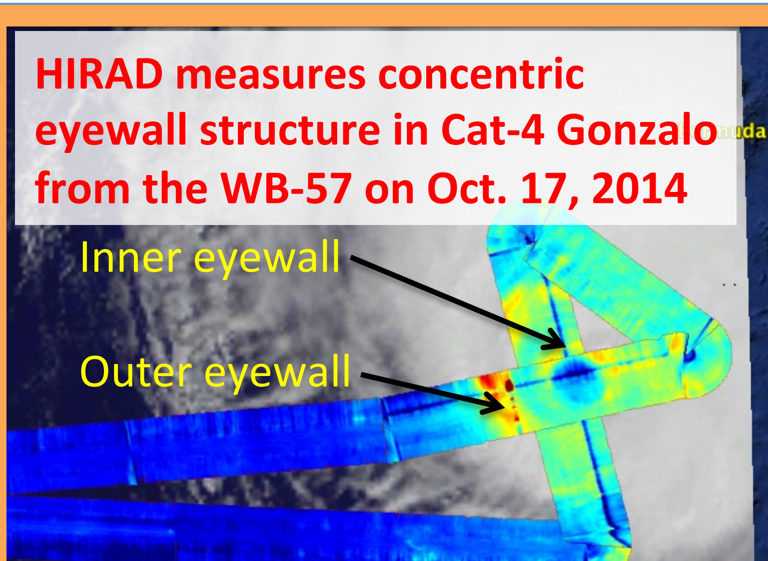

HIRAD measures concentric eyewall structure in Cat-4 Gonzalo from the WB-57 on Oct. 17, 2014

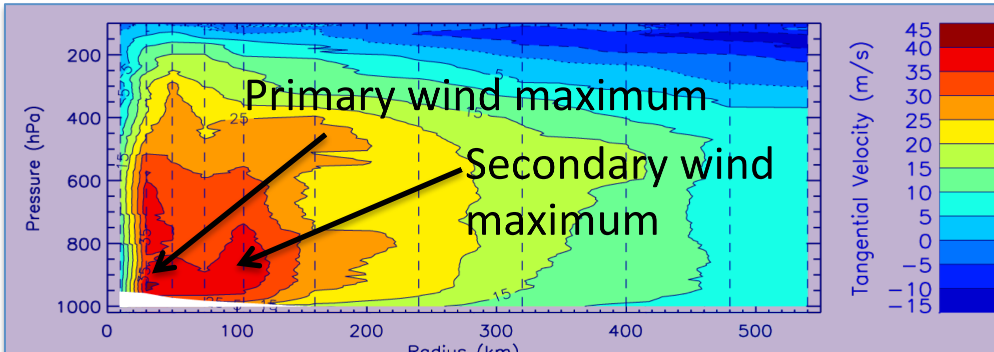

Composite tangential winds on Sept. 16-17 show a developing secondary wind maximum during the formation of a concentric eyewall pattern

Name: Scott Braun, NASA/GSFC, Code 612
E-mail: scott.a.braun@nasa.gov
Phone: 301-614-6316

Data sources: Data from the HS3 2014 field campaign are shown and include information from the Cloud Physics Lidar (CPL), Scanning High-resolution Interferometer Sounder (S-HIS), dropsondes from the Airborne Vertical Atmospheric Profiling System (AVAPS), and the Hurricane Imaging Radiometer (HIRAD). Flights include Hurricane Cristobal (Aug. 26-27 and 28-29), Tropical Storm Dolly (Sept. 2-3), Invest A90L and the Saharan Air Layer (Sept. 5-6), Hurricane Edouard (Sept. 11-12, 14-15, 16-17, 18-19), and two NOAA flights in the Atlantic Main Development Region for tropical cyclones (Sept. 22-23, 28-29).

Technical Description of Figures:

Upper right: CPL and S-HIS data from Sept. 14-15 when Edouard was undergoing rapid intensification into a strong Cat-2 hurricane. CPL data show the cloud tops over the eyewall and outer rain regions, but a sharp drop in cloud heights during passage over the eye. A dropsonde released into the eye and lower eyewall found a surface pressure of 967 hPa and wind speed of 40 ms-1 (77 kt) suggesting that the minimum pressure in the center was probably closer to 960 hPa. The values were ~10 hPa and ~10 kt greater than measured 4 hours earlier by a NOAA P-3.

Lower right: Composite radial cross section of tangential wind from all 88 dropsondes during the flight of Sept. 16-17 when the storm was near maximum intensity. The strongest winds are in the eyewall near 30 km and a weaker secondary maximum is seen near 100 km. During this time and later, satellite imagery showed a clear secondary eyewall, forming concentric eyewall structures.

Lower left: HIRAD "excess" (above the modeled value) brightness temperatures for Hurricane Gonzalo on Sept. 17, showing a concentric eyewall pattern. These brightness temperatures will, in the months ahead, be converted into surface wind speed and rainfall.

Scientific significance, societal relevance, relation to future missions: The Global Hawk provides a valuable capability for mapping out large regions of the storm and its environment. Despite being a relatively quiet season, HS3 was able to take measurements in 4 named storm, including 2 major hurricanes. The Hurricane Edouard flights sampled the majority of Edouard's life cycle, from initial tropical storm, through rapid intensification, and eventual rapid weakening. The Gonzalo flights with the WB-57 (the "over-storm" Global Hawk failed to make it to Wallops for a second year, forcing HS3 to move HIRAD and HIWRAP to the WB-57) provided HS3's first good over-storm measurements for a hurricane and will provide valuable information on concentric eyewall structure. This work provides a significant set of observations for understanding how the large-scale environment (including Saharan air) impacts developing storms and can provide important information for the analysis of data in hurricanes from satellite data such as from TRMM, GPM, Aqua, CALIPSO, and NPP.

Assimilating Data from the Global Hawk Improves Hurricane Forecasts

Jason Sippel, Lin Tian, Gerry Heymsfield, and Scott Braun

Code 612, NASA/GSFC, GESTAR

Observed and predicted maximum winds from Hurricane Karl

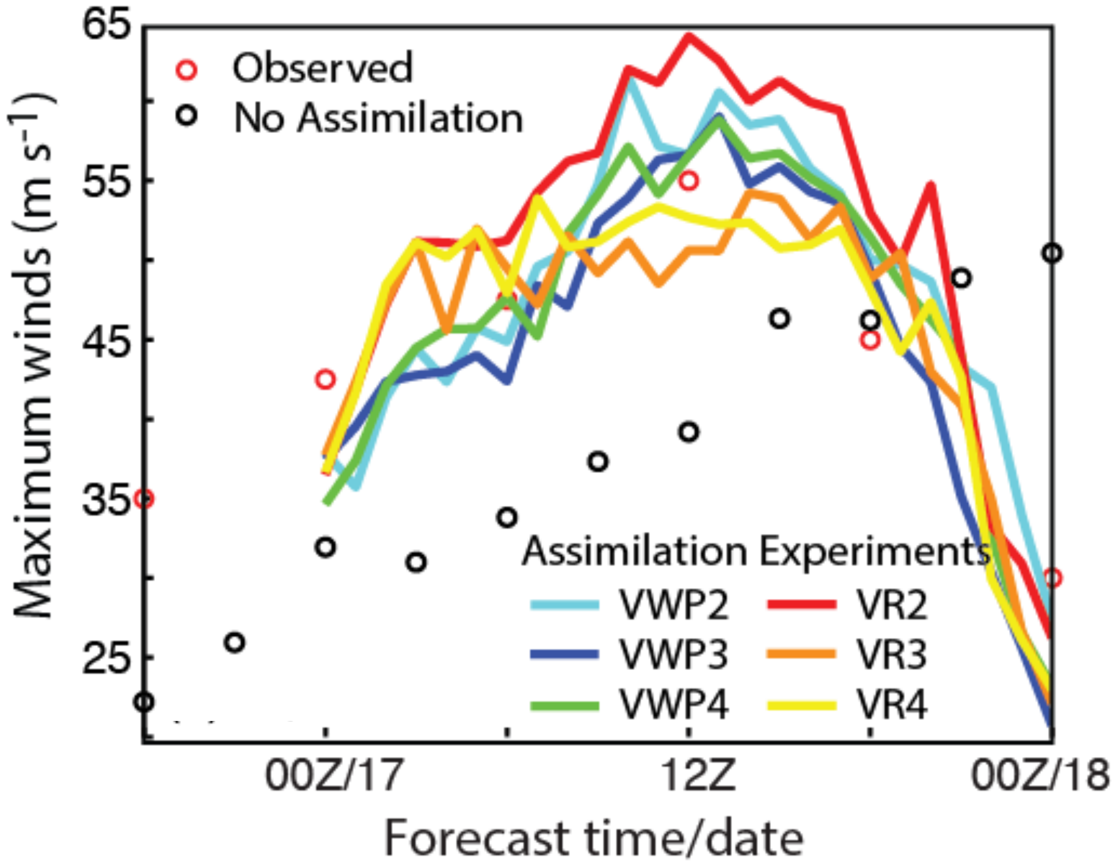

Assimilating data from NASA's HIWRAP radar, which was on the Global Hawk during the GRIP experiment in 2010, significantly improves forecasts of Hurricane Karl. The image on the left shows the evolution of observed maximum winds compared to those in forecasts with and without assimilation. All six assimilation experiments show large improvements upon the experiment without assimilation.

Name: Scott Braun, NASA/GSFC, Code 612
E-mail: Scott.A.Braun@nasa.gov
Phone: 301-614-6316

References:

Sippel, J. A., F. Zhang, Y. Weng, L. Tian, G. M. Heymsfield, and S. A. Braun, 2014: Ensemble Kalman Filter Assimilation of HIWRAP Observations of Hurricane Karl (2010) from the Unmanned Global Hawk Aircraft. *Mon. Wea. Rev.,* **142,** 4559-4580.

Data Sources:

High-altitude Imaging Wind and Rain Airborne Profiler (HIWRAP) data from Hurricane Karl, taken during the Genesis and Rapid Intensification Processes (GRIP) experiment during 2010.

Technical Description of Figures:

Graphic 1: The evolution of observed maximum winds compared to that from a forecast without assimilation and from forecasts initialized from ensemble Kalman filter analyses at UTC 17 September 2010. Three of the experiments shown assimilated HIWRAP Doppler velocity (Vr) observations, and the other three assimilated HIWRAP-derived horizontal wind profiles (i.e., VWPs). The number in the experiment name (i.e., “2” in “VR2” or “VWP2”) indicates the assumed observation error for the experiment. For both Vr and VWP, observation error values of 2-4 m/s were tested.

Scientific significance, societal relevance, and relationships to future missions: The results show that data from unmanned aircraft can potentially be used to improve hurricane forecasts in the future. Since the Global Hawk has a maximum flight duration of about 26 h, which is two to three times that of other hurricane-observing aircraft, there are several significant advantages to using the plane as a hurricane reconnaissance system. For example, it can reach tropical cyclones much farther from land than other aircraft are capable of reaching. For cyclones close to land, the Global Hawk can remain on station much longer, which could provide near constant monitoring. This advancement is most beneficial forecasts of tropical cyclones in data sparse locations or during periods of large forecast uncertainty and intensity change. Current plans are for the National Oceanographic and Atmospheric Administration to use the Global Hawks for hurricane reconnaissance in 2015 and 2016.

Using MODIS cloud regimes for understanding radiation and rainfall budgets

L. Oreopoulos, N. Cho, D. Lee (Code 613), G. J. Huffman (612), and S. Kato (LARC)

Maps of the frequency of occurrence of the MODIS cloud regimes shown to the right

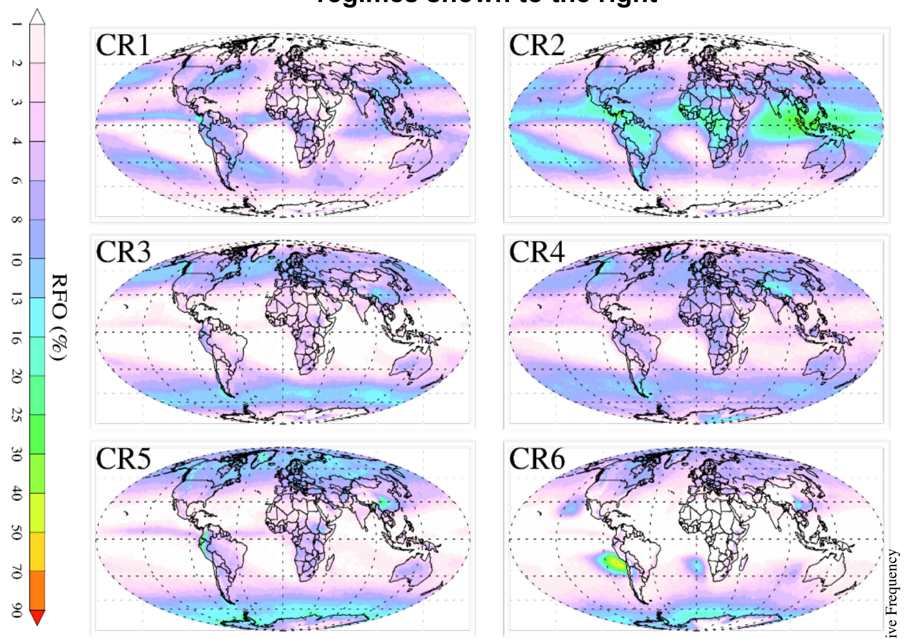

Mean joint histograms of 6 (out of 10) MODIS cloud regimes from clustering analysis

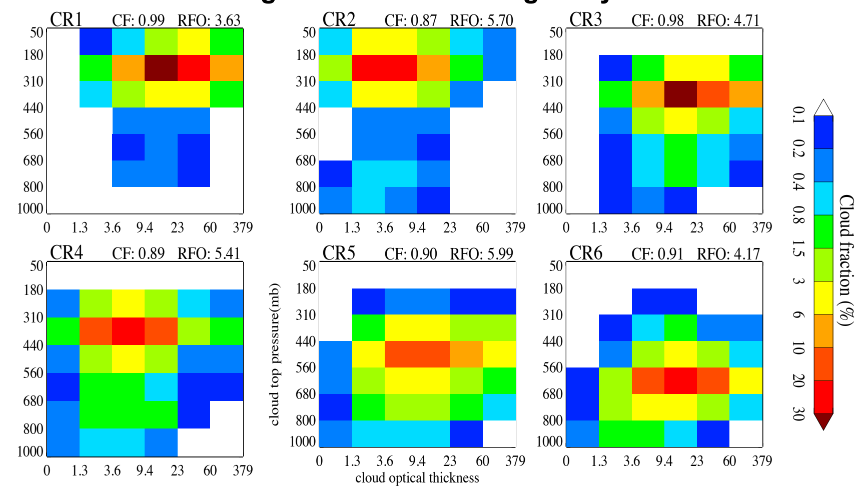

Rainfall histograms of MODIS regimes

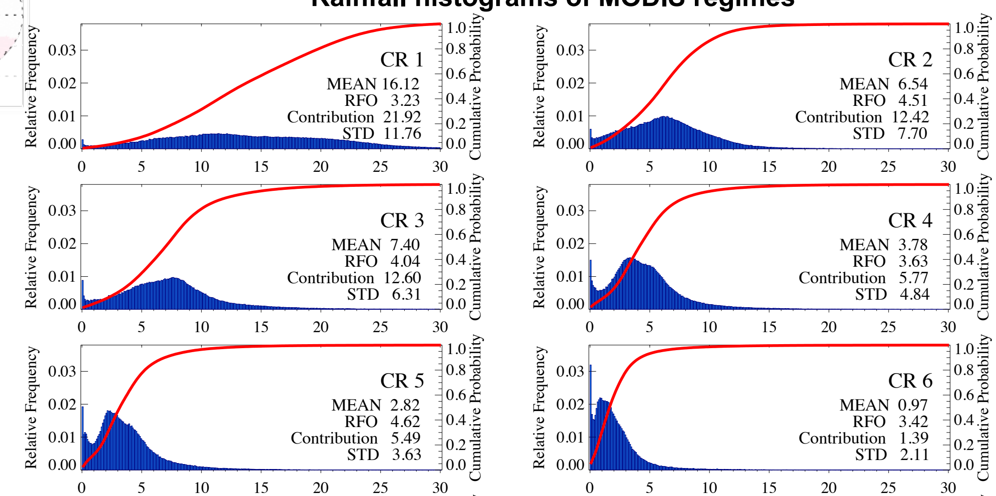

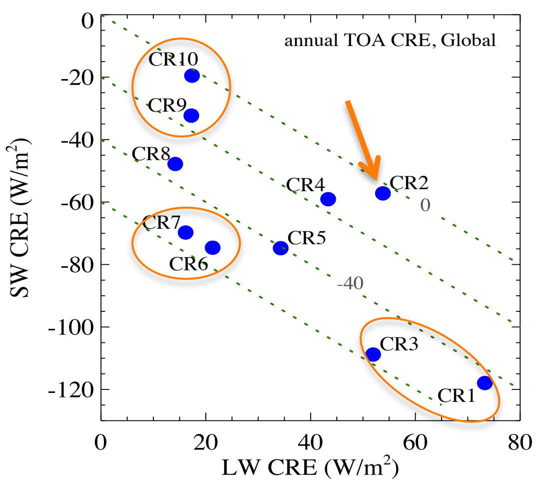

SW and LW Cloud Radiative Effect of MODIS regimes

Our analysis elucidates how much different mixtures of cloud types, as represented within MODIS cloud regimes, contribute to radiative fluxes and precipitation

Name: Lazaros Oreopoulos, NASA/GSFC, Code 613
E-mail: Lazaros.Oreopoulos@nasa.gov
Phone: 301-614-6128

Reference: Oreopoulos, L., N. Cho, D. Lee, S. Kato, and G. J. Huffman (2014), An examination of the nature of global MODIS cloud regimes, J. Geophys. Res. Atmos., 119, doi:10.1002/2013JD021409.

Data Sources: About 10 years of MODIS (Terra and Aqua) daily Level-3 1 degree cloud optical properties from Collection 5.1, mainly joint histograms of cloud optical thickness and cloud top pressure. For the same time period we also use spatiotemporally matched CERES radiative fluxes (SYN1deg) from which the cloud radiative effect is derived, and GPCP daily 1 degree surface precipitation estimates. The paper referenced above also uses a plethora of measurements from the A-Train (CloudSat, CALIPSO, AIRS) as well as MERRA re-analysis data, not shown here, which help us probe deeper into the nature of the MODIS cloud regimes.

Technical Description of Figures (clockwise from top):
Multipanel Map Graph: The geographical distribution of the multiyear mean relative frequency of occurrence of each of the first six (out of ten) MODIS cloud regimes from combined Aqua and Terra data**.** The maps essentiall show how likely or unlikely it is to encounter in a particular location the MODIS regimes represented by the joint histograms to the right.

Multipanel 2D Histogram Graph: The first six (out of ten) MODIS cloud regime centroids (mean histograms) as derived from k-means clustering analysis on the combined Aqua-Terra MODIS 1° joint cloud optical thickness/cloud top pressure histograms. These can be thought as representing six of the main cloud mixtures as observed by MODIS. We provide for each regime the multiannual globally averaged relative frequency of occurrence (RFO) and the mean total cloud fraction derived from compositing MODIS total cloud fractions of successful retrievals.

Multipanel 1D Histogram Graph: GPCP-based histograms daily precipitation rate and corresponding cumulative frequency curves (with scale given in the right ordinate) for the six MODIS cloud regimes. Each panel also shows each regime's mean precipitation rate, its contribution to the global precipitation, the standard deviation of all available gridcell daily values ("STD"), and its relative frequency of occurrence (RFO). The statistics include zero values of precipitation not shown in the histograms themselves.

Graph with isolines and blue dots: The global multi-annual mean shortwave (SW) and longwave (LW) cloud radiative effect CRE (difference between all-sky and cloudless sky radiative fluxes) of each of our ten MODIS cloud regimes (only six of which are shown in the other graphs here). The dashed lines running diagonally represent constant net=SW+LW CRE

Scientific significance, societal relevance, and relationships to future missions: The concept of cloud regimes as defined in the current work is now about 10 years old. The ever-growing body of work built around it demonstrates its acceptance as a promising approach for making sense of a wide range of processes affecting and being affected by clouds. The present study serves as one more affirmation that cloud regimes derived from cluster analysis of passive satellite retrievals at scales around 100 km are an appropriate foundation for decomposing the Earth's water and energy budget in a meaningful way. By examining, with the aid of satellite simulators, the extent to which GCMs can replicate these regimes we can identify model deficiencies and ultimately improve cloud representations. The regimes also provide an appropriate framework to meaningfully compare the consistency between passive and active cloud observations, guiding thus decisions on measurement capabilties for future cloud-oriented satellite missions.

Excellent Agreement of Total Column Ozone Retrievals from the Pandora Spectrometer System and Dobson Spectrophotometer in Boulder Colorado

Jay Herman (UMBC/JCET, Code 614) and Collaborators

Pandora: A much less expensive, but more capable instrument than the traditional Dobson Spectrophotometer or Brewer Spectrometer

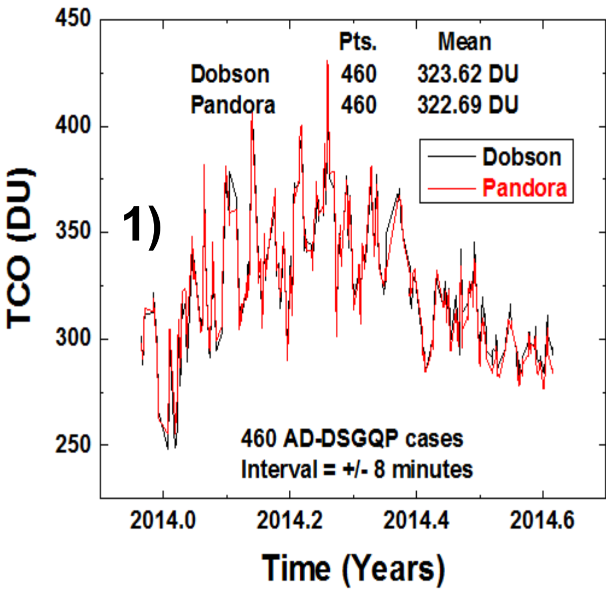

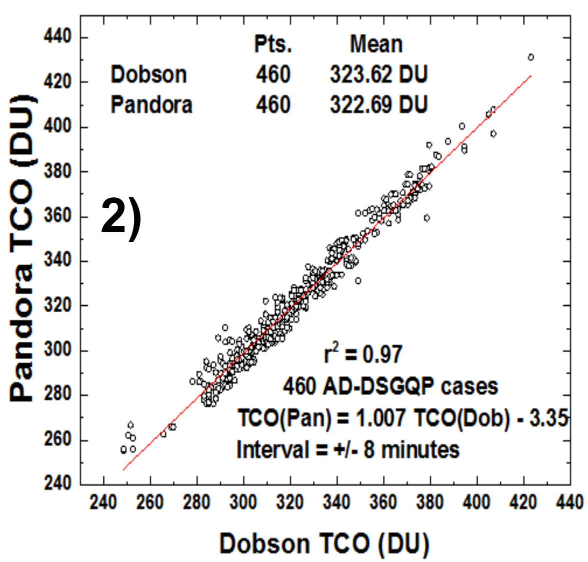

Comparison of ozone values obtained from Dobson-61 compared to Pandora 34 with both operating on the NOAA building in Boulder Colorado

The growing set of 37 Pandora instruments are located at various places in the US, Asia, and Europe and can be used for the validation of satellite data for ozone and NO_2 as well as determining local air quality.

Name: Jay Herman, Code 614 and UMBC
Email: jay.r.herman@nasa.gov
Phone: 301-614-6039

Data Source: Submitted for publication: A NASA developed Pandora Spectrometer system was installed on the roof of the NOAA building in Boulder, Colorado for the purpose of comparing measured total column ozone amounts TCO with a well calibrated classic Dobson spectrophotometer system. The Dobson system has been a worldwide standard ozone measuring device for more than 50 years that requires manual operation to make measurements a few times per day. The Pandora system is automatic, both for data acquisition and data processing, and can make measurements every 40 seconds for ozone ant other atmospheric trace gases. The results of the comparison campaign (December 17, 3013 – September 24, 2014) showed excellent agreement within 2% for all-sky conditions and within 1% for clear-sky days. The day to day variation measured by the two systems also showed very high statistical correlation. The results imply that the fully automated Pandora system could be an inexpensive candidate for replacing the labor intensive Dobson instrument.

Technical Description of Figures:
Graph 1 Pandora-Dobson TCO comparisons under Dobson AD-DSGQP clear-sky criteria showing an ozone time series compared with Pandora TCO averaged over +/- 8 minutes of the Dobson retrieval time

Graph 2 Scatter plot Pandora-Dobson TCO comparisons under Dobson AD-DSGQP clear-sky criteria showing the degree of agreement: Correlation of 0.97 and a slope of 1.007

Scientific significance, societal relevance, and relationships to future missions:
The set of 37 Pandora instruments are located at various places in the US, Asia, and Europe and can be used for the validation of satellite data for ozone and NO_2 as well as determining local air quality. These Pandoras are more capable than the traditional Brewer and Dobson instruments, operate autonomously, and are much less expensive. In addition to total column measurements, the Pandoras also provide altitude profiles throughout the day. The Pandora network is rapidly growing with NASA and non-NASA institutions acquiring instruments. Current locations are in Korea, Finland, Austria, Spain, New Zealand, Canada, and the US (Harvard, GSFC, NASA-HQ, Wallops Island, Langley, New Mexico, St Louis, Hawaii-Mauna Loa Observatory). A shipboard version has been developed that was deployed in the Chesapeake Bay and in the Gulf of Mexico during the DISCOVER-AQ campaigns to help determine airborne nitrification of coastal waters. The Pandora instrument has been used to validate AURA/OMI, NPOESS/OMPS, and will be used for the future TEMPO and DSCOVR missions.

Co-Investigators: Jay Herman[1], Robert Evans[2], Alexander Cede[4], Nader Abuhassan[1], Irina Petropavlovskikh[3], Glen McConville[3]
[1]University of Maryland Baltimore County UMBC-JCET Joint Center for Earth Systems and Technology and NASA Goddard Space Flight Center Greenbelt, MD 20771. [2]NOAA Earth System Research Laboratory, 325 Broadway, Boulder, CO 80305
[3]Cooperative Institute for Research in Environmental Sciences, University of Colorado, Boulder 80309